Mössbauer study of FeCoNbBCu hitperm-type alloys

J. S. Blázquez, A. Conde, and J. M. Grenèche

Citation: Applied Physics Letters **81**, 1612 (2002); doi: 10.1063/1.1504164

View online: http://dx.doi.org/10.1063/1.1504164

View Table of Contents: http://scitation.aip.org/content/aip/journal/apl/81/9?ver=pdfcov

Published by the AIP Publishing

Mössbauer study of FeCoNbBCu hitperm-type alloys

J. S. Blázquez and A. Conde[a)]
Departamento Física Materia Condensada, CSIC-Universidad Sevilla, Apartado 1065, 41080 Sevilla, Spain

J. M. Grenèche
Laboratoire de Physique de L'Etat Condensé, Université du Maine, 72085 Le Mans, France

(Received 17 April 2002; accepted for publication 10 July 2002)

FeCoNbBCu alloys have been studied by Mössbauer spectrometry. A high contribution of the interfacial region in the nanocrystalline samples to the hyperfine field distribution is detected. The possible presence of B in the nanocrystalline grains is also discussed. Low values of the hyperfine field with respect to the disordered α-FeCo phase suggest the presence of the ordered α'-FeCo phase. Recrystallization phenomena at the second crystallization stage are confirmed. © *2002 American Institute of Physics.* [DOI: 10.1063/1.1504164]

Nanocrystalline Fe-based alloys in which nanosized grains of a soft ferromagnetic crystalline phase are embedded in a soft ferromagnetic amorphous matrix have been found to be excellent soft magnetic materials. FINEMET alloys (derived from precursor $FeSiNbBCu$[1]) and NANOPERM alloys[2] [FeMB(Cu) with $M=$Zr, Nb, Hf...] have been widely studied and are among the softer magnetic materials known up to now. In both series the addition of about 1 at. % Cu is useful to improve the nucleation process, refining the grain size and thus improving the soft magnetic properties.[3] These outstanding magnetic properties are reduced by increasing the temperature above the Curie temperature of the amorphous phase. HITPERM alloys (FeCoMBCu),[4] due to the partial substitution of Fe by Co, exhibit a higher Curie temperature of the amorphous phase.

^{57}Fe Mössbauer spectrometry is a nondestructive and effective tool to probe the Fe environment in these FeCo-based alloys. Recently, a few studies have been published on Zr-containing HITPERM alloys[5,6] and CoFeNbB alloys.[7] In the present work a series of melt-spun ribbons ($\sim 20\ \mu$m thick and 5 mm wide) of nominal composition $Fe_{78-x}Co_xNb_6B_{15}Cu_1$ ($x=18$, 39, and 60) has been studied at room temperature by transmission Mössbauer spectrometry (^{57}Co source diffused into a Rh matrix) (1) in the as-cast state, (2) at the end of the nanocrystallization process (annealed under argon atmosphere at 10 K/min up to 873 K for the alloys with 18 and 39 at. % Co, or 823 K for the 60 at. % Co containing alloy), and (3) after the second crystallization process (annealed at 10 K/min up to 948 K for the alloy with 60 at. % Co), in which the α-FeCo phase and the amorphous matrix partially recrystallizes into the $(FeCo)_{23}B_6$ phase.[8] The hyperfine parameters were refined using the MOSFIT program. The values of the isomer shifts (IS) are quoted relative to the α-Fe foil at 300 K.

Figure 1 shows the Mössbauer spectra for the studied samples. For the as-cast samples they exhibit magnetic sextets with broadened and overlapped lines, assigned to the structural disorder of the amorphous state. The fitting procedure thus requires a distribution of sextets. In the 18 at. % Co alloy, a small crystalline contribution clearly occurs, which may be associated with surface crystallization of the ribbon,[9] not detected neither by x-ray diffraction (XRD) nor by transmission electron microscopy experiments, because of its small content ($\sim 2\%$) and because of the electropolishing treatment of the two faces of the ribbon, respectively.

The hyperfine field (B_{hyp}) distribution for the nanocrystalline samples (Fig. 2) can be roughly divided into three contributions: crystalline, interface, and amorphous.[10] Results are summarized in Table I. The lower values of the averaged hyperfine field of the residual amorphous matrix in the nanocrystalline samples compared to the as-cast samples must be due to the enrichment of the matrix in Nb and B.[11]

The angle (θ) between the incident γ radiation and the hyperfine field shows similar trends with the Co content of the alloy to the saturation magnetostriction (λ_s).[12] In fact, both λ_s and θ decrease as the Co content increases in the alloy for the as-cast samples, but during nanocrystallization this dependency is reversed, increasing both λ_s and θ as the Co content increases in the alloy. However, no direct correlation between λ_s and θ can be found because λ_s increases after nanocrystallization (except for the 18 at. % Co alloy) but the angle is lower in the nanocrystalline samples than in the as-cast samples, indicating the important effect of the microstructure.

The B_{hyp} range for the crystalline contribution in the nanocrystalline grains is 37.5–33.5 T for the 18 at. % Co alloy, 35.2–32.7 T for the 39 at. % Co, and 34.2–33.0 T for the 60 at. % Co. The broader distribution for the lowest Co content is in agreement with the behavior found in bcc FeCo binary alloys,[13,14] in which a steeper variation of B_{hyp} can be found for the lowest Co content, until 30 at. % Co, where a maximum is reached. After this maximum the decrease is less marked, reaching values lower than 33.0 T for the highest Co concentration explored (~ 75 at. %).[13] Assuming for the crystalline phase the composition estimated by atom-probe experiments,[11] in which the Co concentration is homogeneous throughout the nanocrystalline grains and the amorphous matrix, we can observe the B_{hyp} dependence with the Co content of the nanocrystalline grains. The values obtained are in agreement with those reported in Ref. 14 for binary alloys with 18 and 60 at. % Co. For the 39 at. % Co alloy, we have obtained a lower value. For this alloy, even the full

a)Author to whom correspondence should be addressed; electronic mail: conde@us.es

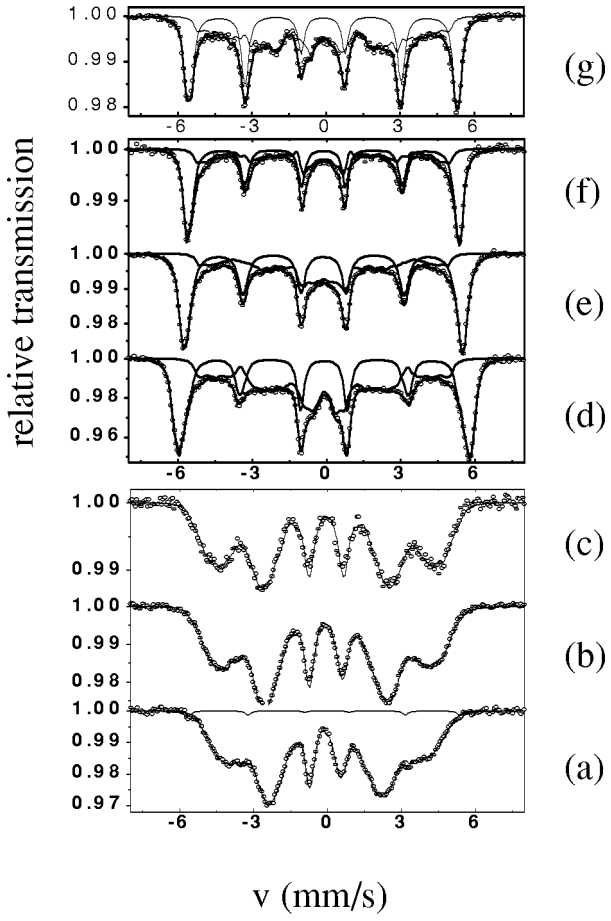

FIG. 1. Mössbauer spectra for as-cast samples (a) 18 at. % Co, (b) 39 at. % Co and (c) 60 at. % Co containing alloys. For nanocrystalline samples (d) 18 at. % Co, (e) 39 at. % Co, (f) 60 at. % Co containing alloys previously heated at 10 K/min up to 873, 873, and 823 K, respectively, and (g) for fully crystallized sample of 60 at. % Co containing alloy, previously heated up to 948 K at 10 K/min.

range of B_{hyp} distribution (32.7–35.2 T) corresponding to the crystalline phase has lower values than those corresponding to the binary alloy. This could be due to the experimental errors, but it is important to note that the values of Ref. 14 correspond to a disordered α-FeCo phase. It was previously observed that the ordered α'-FeCo phase exhibits lower values for B_{hyp}.[13] In fact, if an ordered phase is formed with the nanocrystalline grain composition $Fe_{61}Co_{39}$ (which is in the range of stability for the ordered phase at room temperature[15]), the mean Fe environment changes from the ordered to the disordered phase. As the number of Co first neighbors in the ordered phase is larger, this would result in a lower value of B_{hyp} for this phase. In addition, the behavior of $\langle \mathrm{IS} \rangle$ for the crystalline contribution in the nanocrystallized samples with 39 and 60 at. % Co, showing approximately equal values, agrees with the results found for the ordered α'-FeCo phase, whereas for the disordered phase a continuous decrease is found.[13] The α'-FeCo phase has been experimentally detected in $Fe_{44}Co_{44}Zr_7B_4Cu_1$ HITPERM alloy using synchrotron radiation.[4]

In the nanocrystalline samples an important contribution of the interface is observed (between 14%–20% of the total Fe). This might be due to the small size of the nanocrystalline grains in these alloys (~5 nm).[16] Indeed, if we consider the ratio between the Fe percentage in the pure crystalline phase and the Fe content in the combined crystalline phase and interface, the interface thickness can be estimated at around 0.4–0.6 nm, which is roughly twice the lattice parameter of the bcc α-FeCo phase. Other authors consider that this region of B_{hyp} ranged from ~20 to ~32 T, corresponds to the presence of nonferromagnetic atoms in the nanocrystals (B, Nb).[5] However, our results indicate that the region is more important in these alloys with smaller crystalline grains, that is, higher surface/volume ratio. Atom-probe experiments show rejection of Nb to the matrix, but seems to detect ~5 at. % B inside the nanocrystals,[11] a value much higher than the solubility of B expected in the α-FeCo phase and in contradiction with theoretical predictions.[17] This result, detected in other nanocrystalline compositions by atom probe,[3] could be an artifact, due to the diffusion of B into the nanocrystalline grains during the atom-probe experiment. From Mössbauer experiments it is possible to obtain data which might help to elucidate this problem. Assuming the homogeneity of Co distribution in the material, we have assumed two possible nanocrystalline grain compositions:

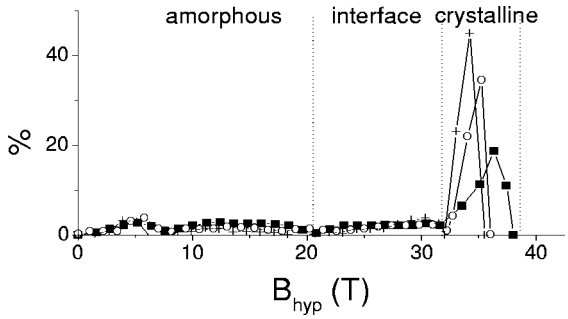

FIG. 2. Hyperfine field distribution for nanocrystalline samples of 18 (squares), 39 (circles) and 60 (crosses) at. % Co alloys, previously heated at 10 K/min up to 873, 873, and 823 K, respectively.

(a) B and Nb are completely rejected from the nanocrystalline grains to the matrix. Thus, the composition of the nanocrystals would be $Fe_{100-x}Co_x$, with x the Co content in the alloy.
(b) The Nb is completely rejected from the nanocrystalline grains, but a residual 5 at. % B remains into the nanocrystals. Thus, the compositions would be $Fe_{95-x}Co_xB_5$.

Usually the crystalline atomic fraction (a_C) is assumed to be equal to the crystalline volume fraction (x_C) and is compared directly with XRD results. However, in these alloys, due to the high B content, the averaged atomic radii in the amorphous matrix and in the crystalline phase are very different. In other nanocrystalline alloys this difference is much smaller: due either to a lower B content in the case of HITPERM[4] and NANOPERM[2] compositions with Zr, to the presence of small atoms in the crystalline phase, such as Si in FINEMET alloys.[1] The expression: $x_C = a_C[\langle R_C \rangle / \langle R \rangle]^3$ (where $\langle R_C \rangle$ and $\langle R \rangle$ are the averaged radii in the crystalline and in the whole alloy, respectively), relates x_C and a_C. If we assume that half of the Fe atoms in the interface correspond to the crystalline contribution we can obtain x_C for the two assumptions proposed (0 and 5 at. % B content in the nanocrystalline grains). The comparison with the XRD data, in which the scattering powers of the two different phases

TABLE I. Hyperfine parameters obtained for the different phases detected (samples identification as in Fig. 1).

Sample	Phase	$\langle B_{hyp} \rangle$ (T)	$\langle IS \rangle$ (mm/s)	θ (degrees)
a	amorphous	22.1	0.023	63.6
b	amorphous	24.2	0.054	62.5
c	amorphous	25.2	0.085	59.2
d	amorphous	11.3	0.056	37.3
	interface	27.1		
	α-FeCo	35.9	0.040	
e	amorphous	10.5	0.047	41.7
	interface	28.0		
	α-FeCo	34.6	0.023	
f	amorphous	8.4	0.020	43.4
	interface	29.5		
	α-FeCo	33.8	0.021	
g	α-FeCo	33.6	0.020	55
	$(FeCo)_{23}B_6$	23.7	0.061	

(amorphous and crystalline) have been taken into account,[16] is presented in Figs. 3(a) and 3(b), assuming 0 and 5 at. % B in the nanocrystalline grains, respectively. It can be observed that a better agreement is obtained under the assumption of complete B rejection from the nanocrystalline grains, but lower values for the Mössbauer experiments have been found. This could be due to an overestimation of x_C by XRD technique, or because the contribution of the interface to the crystalline diffraction phase is more than half of the atoms. In the two cases we have a smaller crystalline fraction for the 60 at. % Co alloy at the end of the nanocrystallization process compared to the other alloys, in agreement with our previous results.[16] This difference was explained in terms of an amorphous matrix exhausted in Fe at the end of nanocrystallization for the 60 at. % Co alloy. In fact, the Fe content

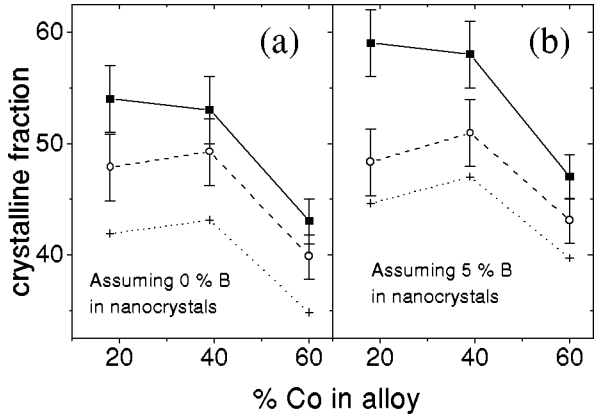

FIG. 3. Comparison between crystalline volume fraction obtained from XRD (squares) and from Mössbauer spectroscopy (circles). Crystalline atomic fraction (crosses) appears for comparison, assuming (a) 0% and (b) 5 at. % B in the nanocrystalline grains.

in the residual amorphous matrix is ~6% of the total atoms, assuming half of the interface contributing to the nanocrystalline grains and complete rejection of the B atoms.

For the fully crystallized sample of the 60 at. % Co alloy it is clear that the number of Fe atoms belonging to the α-FeCo phase decreases. In this process part of the α-FeCo nanocrystalline grains, along with the surrounding amorphous matrix, recrystallizes forming a $(FeCo)_{23}B_6$ phase,[8] which is ferromagnetic at room temperature. This phase is the main boride phase present at this stage, so the parameters obtained from the distribution of B_{hyp} might correspond mainly to this phase. The similar values of $\langle B_{hyp} \rangle$ and $\langle IS \rangle$ found in the nanocrystallized and the fully crystallized samples of the 60 at. % Co alloy, agree with the lattice parameter behavior for the α-FeCo phase, which remains constant after the transformation. The parameters found for the $(FeCo)_{23}B_6$ phase are similar to those found for the as-cast sample. In fact, the composition in Fe, Co, and Nb of the boride phase, measured by windowless energy-dispersive X-ray analysis are very similar to that of the as-cast sample and, therefore, the chemical environment between the initial amorphous and the $(FeCo)_{23}B_6$ phase might be similar. The presence of several different atoms in this phase explains the very broad hyperfine field distribution used, due to the large number of possible different Fe sites.

This work was supported by the Spanish Government and EU FEDER (Project PB97-1119-C02-01 and MAT 2001-3175) and by the PAI of the Junta de Andalucía. J.S. Blázquez acknowledges a research fellowship of the DGES.

[1] Y. Yoshizawa, S. Oguma, and K. Yamauchi, J. Appl. Phys. **64**, 6044 (1988).
[2] K. Suzuki, A. Makino, N. Kataoka, A. Inoue, and T. Masumoto, Mater. Trans., JIM **32**, 93 (1991).
[3] Y. Zhang, K. Hono, A. Inoue, and T. Sakurai, Mater. Sci. Eng., A **217/218**, 407 (1996).
[4] M. A. Willard, D. E. Laughlin, M. E. McHenry, D. Thoma, K. Sickafus, J. O. Cross, and V. G. Harris, J. Appl. Phys. **84**, 6773 (1998).
[5] T. Kemény, D. Kaptás, L. F. Kiss, J. Balogh, L. Bujdosó, J. Gubicza, T. Ungár, and I. Vincze, Appl. Phys. Lett. **76**, 2110 (2000).
[6] M. Kopcewicz, A. Grabias, M. A. Willard, D. E. Laughlin, and M. E. McHenry, IEEE Trans. Magn. **37**, 2226 (2001).
[7] S. N. Kane, A. Gupta, L. Kraus, and P. Duhaj, J. Magn. Magn. Mater. **215–216**, 375 (2000).
[8] J. S. Blázquez, C. F. Conde, and A. Conde, Appl. Phys. Lett. **79**, 2898 (2001).
[9] Y. Q. Wu, T. Bitoh, K. Hono, A. Makino, and A. Inoue, Acta Mater. **49**, 4069 (2001).
[10] M. Miglierini and J. M. Grenèche, J. Phys.: Condens. Matter **9**, 2321 (1997).
[11] Y. Zhang, J. S. Blázquez, A. Conde, P. J. Warren, and A. Cerezo (in press).
[12] J. S. Blázquez, V. Franco, A. Conde, M. R. J. Gibbs, H. A. Davies, and Z. C. Wang (in press).
[13] B. DeMayo, D. W. Forester, and S. Spooner, J. Appl. Phys. **41**, 1319 (1970).
[14] H. H. Hamdeh, J. Okamoto, and B. Fultz, Phys. Rev. B **42**, 6694 (1990).
[15] O. Kubaschewski, in *Iron-Binary Phase Diagrams* (Springer, Berlin, 1982), pp. 27–31.
[16] J. S. Blázquez, V. Franco, C. F. Conde, and A. Conde (in press).
[17] A. R. Yavari and O. Drbohlav, Mater. Trans., JIM **36**, 896 (1995).